Dynamic Analysis of Bare Printed Circuit Board under Impact

Ahmad H Youssef and Xuejun Fan
Department of Mechanical Engineering
Lamar University
PO Box 10028, Beaumont, TX 77710, USA
xuejun.fan@lamar.edu

Abstract

This paper presents the fundamental understandings of the printed circuit board (PCB) dynamic behaviors under impact loading, with the use of finite element analysis for different configurations of boards. The effects of boundary conditions, and the impulse duration are also investigated. Excellent agreement is obtained between the bare board analysis and the actual component performance for the current JESD22-B111 drop test board. Then the same methodology is extended to a square-shape board. The guidelines for the future component placement and the selection of board dimension and component size are discussed. Fundamental frequencies of the different board configurations are calculated and compared. In addition, new impulse profile is proposed to obtain the board dynamic responses without ringing effect. This new impulse profile provides much convenience in the future for the analysis of drop test related failures.

Introduction

A board level drop test method, JESD22-B111 [1], has been standardized to evaluate the performance of integrated circuit (IC) packages under standard drop conditions. Various shock/impact modeling techniques have been developed to predict board dynamic strains and transient solder joint stresses. The so-called input-G method has been widely adopted since it decouples the board finite element model from the system model [2]. There are several approaches in implementing the input-G method, such as explicit dynamics analysis using DYNA-3D [3], large mass method with implicit dynamics [4], and the input-D method, in which the acceleration input is integrated twice to obtain the displacement boundary condition over time [5]. Mode superposition method is also applied effectively for a linear system under impact loading [6]. Shen and the authors introduced the direct acceleration input (DAI) method as an alternative to apply the impulse loading while removing the rigid body motion. In this method, the acceleration impulse is applied as body forces to the problem under study [7-11]. There are a number of special numerical treatments developed in finite element models to reduce the problem sizes, such as equivalent layer model for solder interconnects [12], shell element application in global models [10], shell-to-solid sub-modeling using beam-shell-based elements [13]. When the details of the components are considered, the finite element model sometimes becomes very big. It is inconvenient to run a parametric study with a detailed finite element model.

In this paper, the bare printed circuit board, i.e., a board without component attachment, is used for dynamic analysis by finite element analysis. Different configurations, including geometry and boundary conditions, are considered. JESD22-B111 rectangular-shape board and the newly proposed square-shape board are investigated. In addition, the effect of screw-type and line-wedge support is studied. The impulse duration is also studied in this paper.

Problem Statements

Two configurations of the bare board are considered, as shown in Figure 1 and Figure 2, respectively. The first configuration is based on the geometry of the JESD22-B111 drop test board, with a dimension of 132mm×77mm×1mm. The span between the screw supports is 99mm and 65mm in short and long board directions, respectively. The diameter of the screw hole is fixed as 3.2mm. The second configuration is of the newly designed square shape [14] with 1mm thickness, with the center of the screw from edge fixed as 3mm. The dimension of the square shape board can be changed.

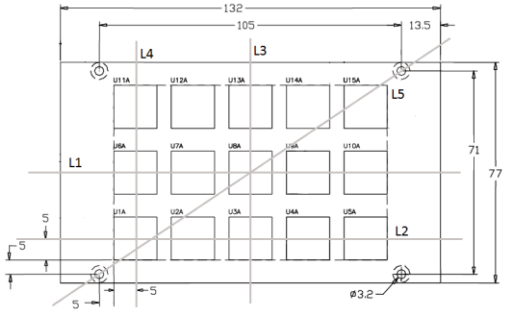

Figure 1 JESD22-B111 drop test board

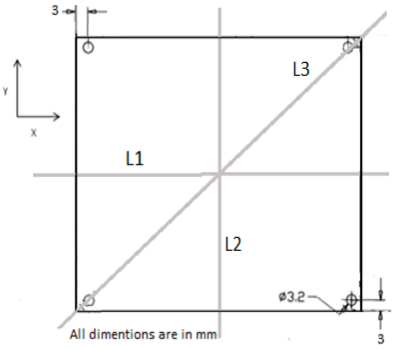

Figure 2 Square-shape board with four-screw support [14]

Two boundary conditions are studied for the square-shape board. The first boundary condition is the screw-type support that is used in current JESD22-B111 drop test. The second boundary condition is a line-wedge support [15], which is considered as a simply supported beam boundary condition, as shown in Figure 3. For the screw-type support, the displacement at the hole surface is fixed in all directions in our finite element analysis.

978-1-4673-1681-1/12/$31.00 ©2012 IEEE

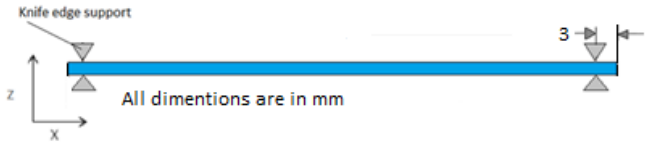

Figure 3 Square board with line-wedge support

We will also study the effect of the impulse duration. According to the Condition B in JESD22-B111, the input acceleration to the board is of half-sine shape, with 1500g peak and 0.5 ms duration, as shown in Figure 4. This impulse profile induces the board to vibrate in several cycles before the rest. We will propose a new impulse condition.

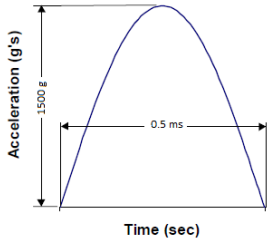

Figure 4 Impulse profile defined by JESD22-B111 drop test

Experimental Validations of Finite Element Model

The damping coefficient of the PCB used in the finite element analysis is calibrated through board strain history measurement. Figure 5 shows the overall comparison of entire strain history during impact, with a damping coefficient of 0.03. The damping coefficient is then used to predict the board dynamic behaviors under various conditions.

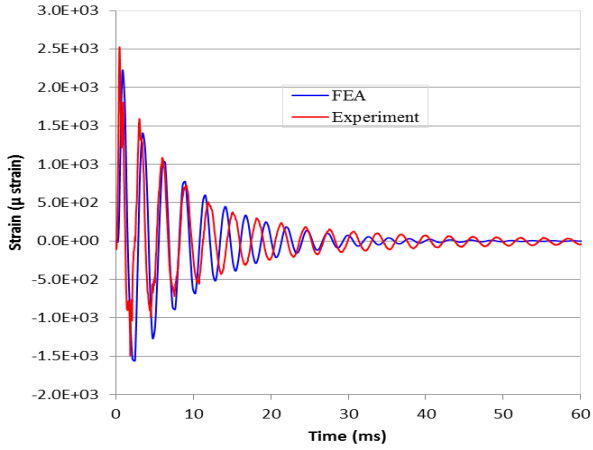

Figure 5 Comparison of bare board strain history

Results of Fundamental Frequencies

Table 1 gives the simulation results of the first four fundamental frequencies of the current JESD22-B111 bare board and the square-shape board with different dimensions. Three dimensions of the square board: 3"×3", 4"×4", and 5"×5", respectively, are modeled. It can be seen,

1. The first fundamental frequency of the current JESD22-B111 bare board is around 231 Hz. Since the components attached to the board are relatively light and small (<15mm), the bare board frequency is very close the frequency with the components 212 Hz [9]. Therefore, the bard board frequency is a good representative value for the actual board with component attachment.
2. For the square-shape board, the first fundamental frequency ranges from 128 Hz to 393 Hz for screw-type support, and from 103 Hz to 287 Hz for wedge-type support, respectively The smaller the board is, the higher the frequency is. In addition, the wedge-type support gives lower frequency than the screw-type support. However, it will be shown later that the wedge-support board introduces larger board deformation (strain) under impact.
3. For the square-shape board, the second and third modes are symmetric with screw-type support. The bend mode shapes are shown in Figure 6.

Table 1 Fundamental frequency results

Freq-uency (Hz)	JESD22 -B111	Square shape					
		3" x 3"		4" x 4"		5" x 5"	
		Screw	Line-wedge	Screw	Line-wedge	Screw	Line-wedge
1	232	393	287	213	165	128	103
2	398	722	483	399	277	243	174
3	561	722	1027	399	595	244	378
4	612	826	1156	463	665	285	417

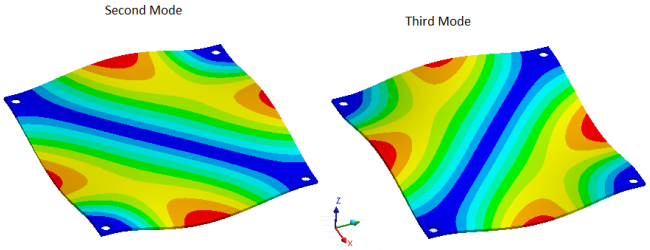

Figure 6 Second and third bend mode shapes for square board with screw-type support

Results for JESD22-B111 Drop Test Board

Previously, board strain analysis and solder joint stresses have been analyzed mainly with components [7-11,16]. In the following, the results from the bard board model will be presented to correlate with the component behaviors in the actual test board. For the convenience of analysis the following lines are defined across the JESD22-B111 board to obtain the strain distributions,

1. Line 1 and Line 2 are defined in the long direction of the board, as shown in Figure 1. These two lines cross all the components to be mounted according to the JEDEC requirements;
2. Similarly, Line 3 and Line 4 are defined in the short direction of the board, as shown in Figure 1, to cross all the components in the short direction.
3. Line 5, which connects along diagonal direction between two screw centers, is also defined.

Figure 7 plots the x-strain distributions (strain in long direction) in Line 1 and Line 2, respectively. The strains are taken at the time when the board reaches the maximum bend mode downward in the first half of the period. The figure shows that in the center of the board, the board bends

downward, with the maximum bend strain at the center. However, in the two ends near screw supports, the board bends in the opposite direction, with the absolute strain value comparable to the one in the center. Please note this strain distribution is in the first peak mode during the first half of the period. In the second-half of the first period, the board center will bend upwards, while the region near screw support will bend downward. From these results, it can conclude that

1) Board strain near edge along Line 2 is comparable to the center strain, but in the different directions. This means that the components mounted near screws , e.g. group A defined JESD22-B111, may fail as quickly as those in the center (e.g. Group E and F) (for group numbers and labels, refer to the JESD22-B111 standard [1]).

2) The strain near edge along Line 2 is significantly less than that in Line 1. This means that the components (e.g. Group C) may fail much slower.

3) The maximum strain at the center along Line 1 and Line 2 are very close. Therefore, Groups F and E will have similar failure rate.

4) The strain along L1 and L2 decreases as the distance from center increases. Thus, Group B or D would expect have less failure rate.

These findings are all in good agreement with previous analysis based on the actual board with component attachment [7-11, 16].

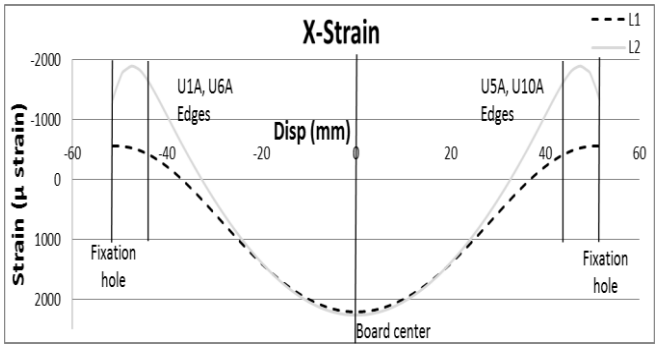

Figure 7 X-strain at Line 1 and Line 2 in the JESD22-B111 bare board

Figure 8 gives the y-strain distributions in Line 3 and Line 4, respectively. From this figure it clearly shows that the strain stays in a relatively flat value along the Line 3. But along Line 4, there are large strains at the two ends, but little strains at the center. These results again confirm the results mentioned above and correlate well with components results.

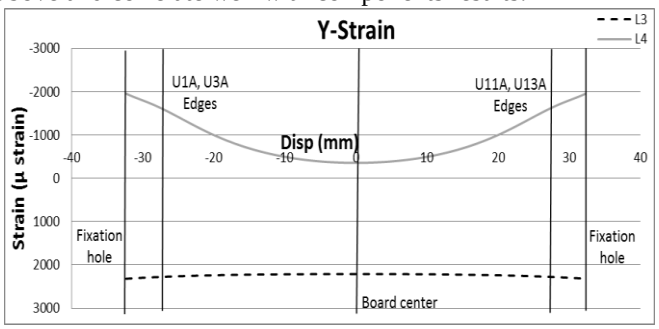

Figure 8 Y-strain Line 3 and Line 4 in the JESD22-B111 bare board

Figure 9 plots both maximum and minimum principal strain distributions in the diagonal direction along Line 5. It clearly shows the effect of screw support, where the absolute value of strain can be significantly higher than the center strain. When the board bends downward, solder joints will be in tensile state for the face-down component attachment [11]. This means that in the second half of the peak mode of the first period, the board will bend downward near screw region while the board center bends upward. Previous work showed that the corner components U1 (group A) will fail earlier than the center component if the component size is small [9]. The results from the bare board can give useful information without involving detailed FEA with components. It has been recommended that the component should be placed far away from the region near screws to avoid excessive stresses due to the excessive bend strains in this region. In addition, it has been found that the distance between the screw and nearby components will have significant impact on the component stress. Therefore, in designing a drop test board, the screw region should not be used for the component attachment.

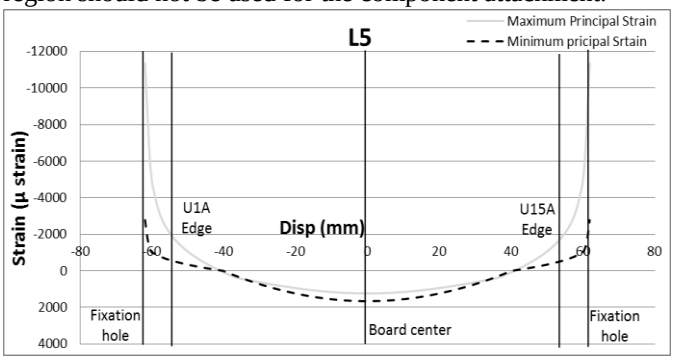

Figure 9 Line 5 Maximum and minimum principal strains

Results for Square-Shape Board

It is suggested that modifying the standard JEDEC board to more symmetric and simple version can increase the efficiency of test and analysis [17]. In this study, three square-shape board sizes are considered. Since the board is symmetric in both x and y direction, for the convenience of analysis, only three lines are defined to analyze the strain distributions: Line 1 and 2, in the center of board, and Line 3, which connects along diagonal direction, as shown in Figure 2. Since the results for Line 1 and Line 2 are symmetric, only the results for Line 1 are presented below for screw-type supports.

Figure 10 plots the x-strain distributions (in x direction) along Line 1, for 3, 4 and 5 inch boards, respectively. It can be seen that with the increase of the board size, the structure tends to be more flexible, and therefore larger bending strain is induced, though the frequency tends to decrease (see Section 4). In addition, the 'edge' effect due to the screws is present to cause board bend in the opposite directions. Figure 11 plots both the maximum and minimum principal strains along the Line 1. It is noted that along Line 1, which is in the middle of the board, the principal bending strain in in one direction only. However, as shown in Figure 12, along the diagonal Line 3, reversed bend occurs near the screw supports. From Figure 12, it can been seen, due to the symmetry, the maximum and minimum principal strains are

almost same due to the zero shear strain along those lines. Excessive bend strain in the opposite direction to the center strain is observed for the square-shape board.

Based on the results from Figures 10 and 11, 12, Figure 13 plots the approximate region where the components might be placed (in yellow color), for the 3"×3" square-shape board. Outside this zone is possible that the effect of the reversed bending will occur. If multiple components are to be used, they cannot overlap each other, therefore, an inner circle can also be defined, as shown in Figure 13. From this analysis, the maximum component size must be less than 22mm for this board if multiple components are placed. The actual allowable component size will be even smaller to eliminate the interactions between adjacent components. If only one component is used and is placed in the center, the maximum size of the component can be very large.

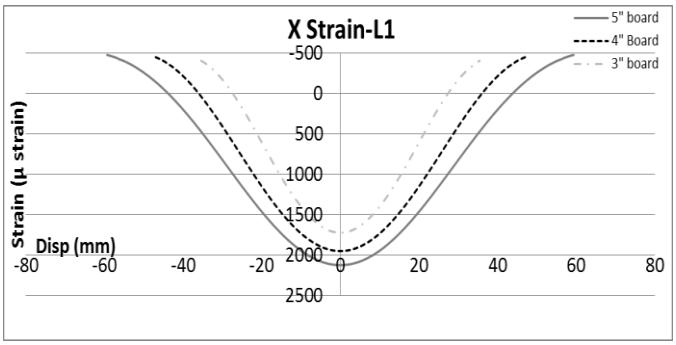

Figure 10 Line 1 X-strain (3x3, 4x4 and 5x5 boards)

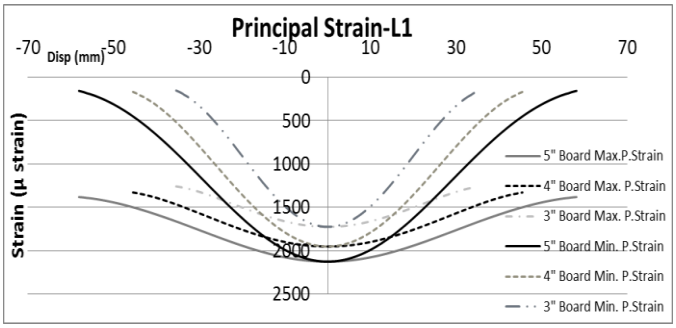

Figure 11 Line 1 Maximum and minimum principal strains (3x3, 4x4 and 5x5 boards)

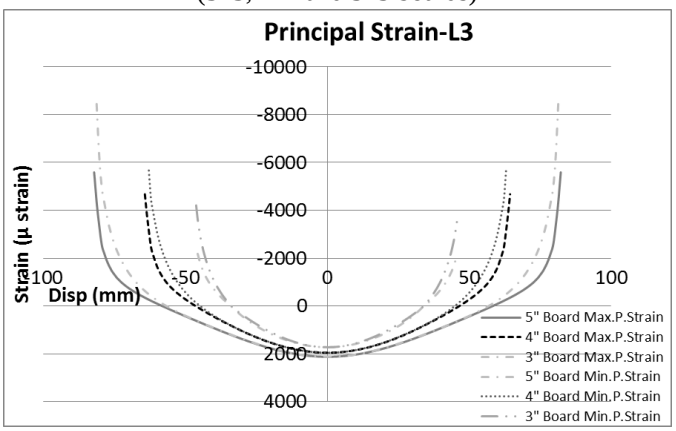

Figure 12: principal strains along L3

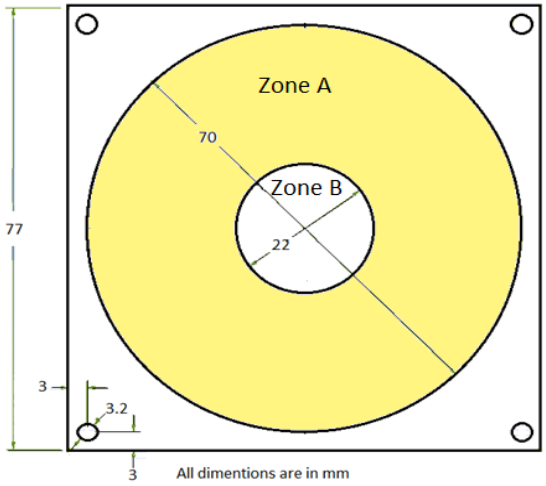

Figure 13 Allowable zone for components placement

Effect of Boundary Conditions

In the following section, the results from the square-shape board, with conventional four screw support will be compared with, a square-shape board, having the new suggested line-wedge support, shown in Figure 3. Figure 14 and 15 plots the maximum and minimum principal-strain distributions in Line 1 and 2 respectively.

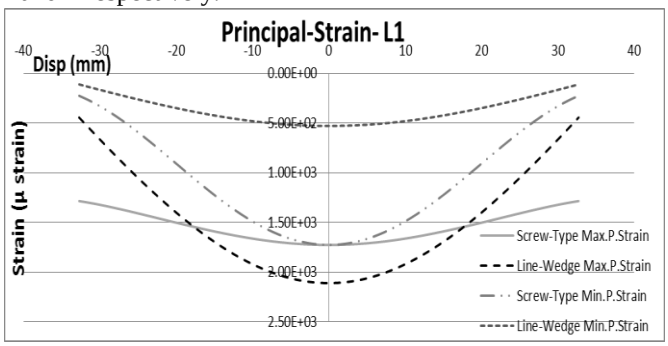

Figure 14 Line 1 Maximum and minimum principal strain for both BCs

From this figures it clearly shows that the strain stays in a relatively flat value along the line 2 for the line-wedge support. This is due to the line support which is in lateral direction. But for screw-type support, there is strain difference between board center and its ends. Strain is higher in line-wedge support and more uniform, with less dependence on the location of component.

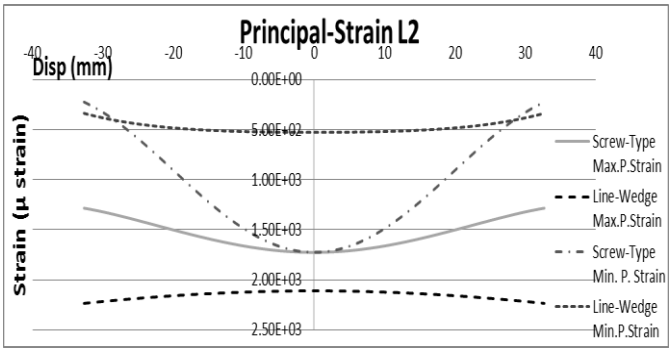

Figure 15 Line 2 Maximum and minimum principal strain for both BCs

Figure 16 plots principal strain distributions in the diagonal directions along Line 3. It clearly shows the difference between these two boundary conditions , on the edge region. For screw-type support the absolute value of strain can be significantly higher than the center strain (in the opposite direction). But line-wedge support does not cause the reversed bend at the edge.

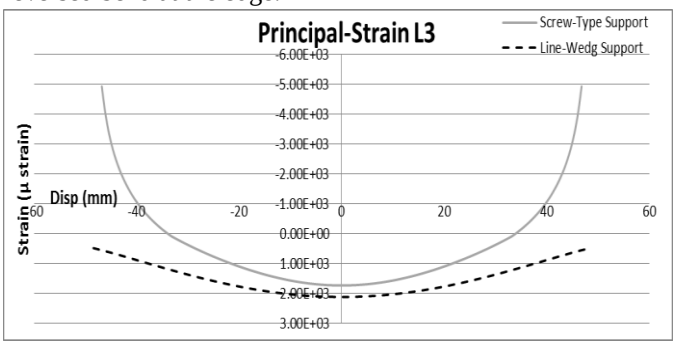

Figure 16 Line 3 Maximum and minimum principal strain for both BCs

Effect of Impulse Duration

Current JESD22-B111 drop test standard requires the impulse duration of 0.5ms. Under this condition, as seen in Figure 5, the board will vibrate several cycles before it comes to rest due to the damping effect. For a one degree-of-freedom model, the analytical solution is available for an impulse profile defined in Figure 4. It has been shown [18, 19] that when the impulse duration is 1.5 times of the system's period, the output response becomes a single period of an amplified dynamic response, and the rest of the response is close to zero. In fact, the analytical solution shows that the certain input pulse time results in no ringing response. For the half-sine input, the no ringing conditions are that the impulse duration $= (i + ½)/f_n$, where i = 1, 2, 3, ... , and f is the fundamental frequency. The smallest duration is 1.5 times of the system's period.

For the drop test board studied here, since the system has infinite number of the degree of freedom, there is no analytical solution available. However, when the impulse time is close to the 1.5 times of the first fundamental period (1/f), we expect to see the output results with very small ringing. When applying 6.4ms impulse duration, Figure 17 shows the output responses, compared to the 0.5ms duration impulse. It clearly shows that the board will only vibrate once with a large amount of deformation, followed by the nearly rest of the board. This will greatly simplify the test results and the subsequent failure analysis. The impulse duration can be controlled in the testing system to adjust the surface material (felt surface, hardness and thickness) to achieve the desirable impulse profile.

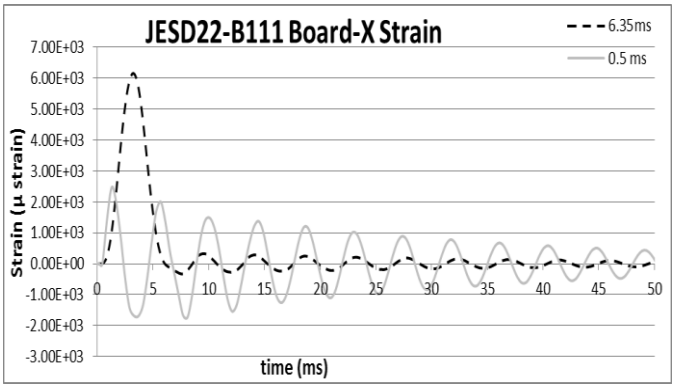

Figure 17 Dynamic response for different impulse durations

Conclusions

The study shows that the bare board analysis can give useful data, which are in a good agreement with full dynamic analysis with components attached. Fundamental understanding of the drop test board behavior can be obtained from the simple bare board finite element dynamic analysis. It adds valuable guides for the component placement in the future in designing new test boards.

References

1. JEDEC Standard JESD22-B111, "Board Level Drop Test Method of Components for Handheld Electronic Products", 2003.
2. J. Luan, T.Y. Tee, "Novel board level drop test simulation using implicit transient analysis with Input-G method", *6th Electronics Packaging Technology Conference (EPTC)*, Singapore, 2004.
3. T.Y. Tee, J. Luan, E. Pek, C.T. Lim, Z.W. Zhong, "Advanced experimental and simulation techniques for analysis of dynamic responses during drop impact", *Proc of Electronic Components and Technology Conference (ECTC)*, pp. 1089 –1094, 2004.
4. A. Syed, M.S. Kim, W. Lin, Y.J. Khim, S.E. Song, H.J. Shin, T. Panczak, "A methodology for drop performance prediction and application for design optimization of chip scale packages", *Electronic Components and Technology Conference (ECTC)*, 2005.
5. S. Irving, Y. Liu, Free drop test simulation for portable IC package by implicit transient dynamics FEM, *Proceedings of the 54th Electronic Components and Technology Conference (ECTC)*, pp. 1062 – 1066, 2004.
6. W.K. Loh, L.Y. Hsiang, A. Munigayah, "Nonlinear dynamic behavior of thin PCB board for solder joint reliability study under shock loading", *International Symposium on Electronics Materials and Packaging*, pp. 268 – 274, 2005.
7. L.X. Shen, "Simulation of drop test board with 15 components using explicit and implicit solvers", *International ANSYS Conference*, Pittsburgh, Pennsylvania, 2008.
8. H.S. Dhiman, "Study on finite element modeling of dynamic behaviors of wafer level packages under impact loading", M.S. Thesis, Lamar University, 2008.

9. H.S. Dhiman, X.J. Fan, T. Zhou, "Modeling techniques for board level drop test for a wafer-level package", *Proc. of International Conference on Electronic Packaging Technology and High Density Packaging (ICEPT-HDP)*, 2008.
10. A.S. Ranouta, "Effects of orientation, layout, component structure and geometry on drop reliability of chip scale packages", M.S. Thesis, Lamar University, 2010.
11. X.J. Fan, A.S. Ranouta, and H.S. Dhiman "Effect of Structure and Material at Package Level on Solder Joint Reliability under Impact Loading", *Transactions on Components, Packaging and Manufacturing Technology*, 2012 (accepted).
12. P. Lall, S. Gupte, P. Choudhary, J. Suhling, "Solder-joint reliability in electronics under shock and vibration using explicit finite-element sub-modeling", *Proceedings of the 56th Electronic Components and Technology Conference (ECTC)*, pp. 428 – 435, 2006.
13. P. Lall, D. Panchagade, Y. Liu, W. Johnson, J. Suhling, "Smeared property models for shock-impact reliability of area-array packages", *ASME Journal of Electronic Packaging*, Volume 129, pp. 373-381, 2007.
14. JEDEC drop test standard JESD22-B111 modification working group, 2012. (Chair: D. J. Xie)
15. Jussi Hokka, Toni T. Mattila, Jue Li, Jarmo Teeri, Jorma. K. Kivilahti, "A novel impact test system for more efficient reliability testing", *Microelectronics Reliability* 50 (2010) 1125–1133.
16. X.J. Fan, A.S. Ranouta, "Finite Element Modeling of System Design and Testing Conditions for Component Solder Ball Reliability under Impact", *Transactions of Components, Packaging and Manufacturing Technology*, 2012 (DOI: 10.1109/TCPMT.2012.2204884).
17. Guruprasad, P., Roggeman, B., Pitarresi, J., "Impact of board configuration and shock loading conditions for board level drop test", *Electronic Components and Technology Conference (ECTC)*, 2011 IEEE 61st, On page(s): 2067 – 2072
18. Niraula, Ratna Prasad, "Study of the drop impact reliability in microelectronics" 2007
19. J. Zhou, "Analytical Analysis on the Effect of Time Duration of Acceleration Pulse to a JEDEC Board in Drop Test", *ICEPT-HDP*, 2008.